www.ietdl.org

Published in IET Power Electronics
Received on 22nd May 2013
Revised on 20th August 2013
Accepted on 21st September 2013
doi: 10.1049/iet-pel.2013.0396

ISSN 1755-4535

Modelling and control of a railway power conditioner in co-phase traction power system under partial compensation

Ning-Yi Dai, Man-Chung Wong, Keng-Weng Lao, Chi-Kong Wong

Department of Electrical and Computer Engineering, Faculty of Science and Technology, University of Macau, Macau, People's Republic of China
E-mail: nydai@umac.mo

Abstract: Co-phase traction power supply system provides continuous power to traction loads without neutral sections. In order to reduce system unbalance, compensate reactive power and harmonics, a railway power conditioner (RPC) operates together with traction transformer in each substation. In the past study, the RPC is designed to achieve three-phase balance and unity power factor (PF) at the grid side. As a result, its rating is high. According to the power quality tariff plan in China, the penalty for reactive power can be avoided if the PF is higher than 0.9. In this study, a grid-side PF of 0.9 is achieved via different control approaches after analysis. Among these approaches, the rating of the RPC in the worst case is more than twice that in the best case. Hence, selection of a suitable control parameter is necessary. The minimum rating of the RPC is achieved by setting the power angle of phases *A* and *B* lagging and the power angle of phase *C* leading under partial compensation. The rating of the RPC is reduced to 70% by setting PF to 0.95 instead of 1. Simulation and experimental results are provided to show the validity of the modelling, design and control method.

1 Introduction

The 25 kV AC system has been adopted in the long-distance electrified railway in many countries. The single-phase traction transformer is widely used in traction substations because of its low cost and simple connection [1, 2]. In order to reduce the imbalance caused by the single-phase traction loads, balance feeding transformers were proposed to replace the single-phase transformer, including Scott transformer, V/V transformer, Y d11 transformer etc. [3, 4]. These transformers have different wiring configurations, but basically they are connected to the three-phase power grid at the primary side and provide two single-phase outputs at the secondary side. Grid-side currents are balanced when the two neighbouring sections supplied by one transformer have the same loading. Practically, system unbalance still exists because of the uneven load distribution. In addition, reactive power and harmonics from the traction loads make the traction transformer work in the derated mode and increase the system losses [5–7].

Co-phase traction power supply was proposed [8–10], which provides continuous power to the locomotives, as illustrated in Fig. 1. By using the railway power conditioner (RPC) to operate together with the balance feeding transformer in the co-phase traction power supply, three-phase balance and unity power factor (PF) are achieved at the primary side [8–12]. The secondary side of the traction transformer, which directly supplies the traction loads, is denoted as loading phase. As a power conditioner, the RPC also changes the active power and reactive power consumption of the loading phase. As a result, the variation of the supply voltage at the loading phase is reduced by the RPC. In addition, harmonics are suppressed by the RPC at the secondary side of the traction transformer.

One of the main obstacles for promoting the co-phase traction power system is the high initial cost of the RPC because of the large-capacity power converters. According to the field recorded data [7], the traction loads vary from 0 to around 40 MW. Previous work indicates that the RPC needs to transfer half of the load active power and provide all the reactive power. In those works, the RPC's rating is calculated in terms of following assumptions [8–12].

- Three-phase currents are balanced at the grid side;
- PF at grid side is unity;
- All the harmonics are compensated.

The above three items are denoted as full compensation in this paper. Based on this setting, the RPC's rating is high. Compensation factors were introduced to let the RPC only provide part of the compensating currents, so that its rating is reduced [13–15]. However, the compensation factors do not directly relate to the system performance, for example, PFs. How to select a proper compensation factor needs further study. In addition, no simple reference current calculation method is proposed when the compensation target varies.

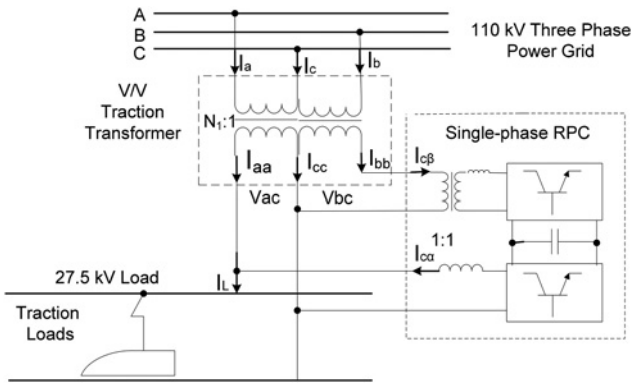

Fig. 1 *Co-phase traction power supply*

In this paper, a method to design the rating of the RPC under partial compensation is studied and the corresponding revised control block is proposed. In Section 2, the mathematical model of the co-phase railway power supply is analysed and the formulas for calculating compensation currents of the RPC in terms of performance index are deduced. Different control approaches of the RPC to achieve the same PF are studied and compared in Section 3. A method to design the RPC with minimum rating and the corresponding control block is proposed in this section. Simulation verifications and experimental results are provided in Sections 4 and 5, respectively. The conclusions are provided in Section 6.

2 Modelling of the co-phase railway power supply

The power quality of the railway power supply system is typically evaluated at the primary side of the traction transformer, that is, the high-voltage grid [5, 16, 17]. The harmonic currents at the secondary side are not able to pass through the traction transformer linearly as the fundamental frequency current does. Harmonics are also better to be compensated at the secondary side to avoid transformer saturation and overheating [18]. Hence, it is assumed the harmonics are compensated by RPC at the secondary side of the traction transformer and are not considered when the performance index is evaluated at the grid side. The fundamental frequency model of the co-phase traction power supply system is discussed hereinafter.

2.1 Model without the RPC

The system configuration of one substation of the co-phase railway power supply is shown in Fig. 1. V/V traction transformer is used in Fig. 1, but other balance feeding transformers are also applicable. The ratio of turns of the traction transformer is N_1. The phasor diagram is shown in Fig. 2*a*, when RPC is not installed. The primary side voltages are denoted as V_A, V_B and V_C; whereas the secondary side voltage is expressed as V_{ac} and V_{bc}. The load current is I_L and load PF is $\cos(\varphi_L)$. The currents at grid side are given in (1), where $\psi_a = \pi/6 = 30^\circ$.

$$\begin{bmatrix} I_a \\ I_b \\ I_c \end{bmatrix} = \frac{1}{N_1}\begin{bmatrix} I_L e^{-j(\psi_a+\varphi_L)} \\ 0 \\ -I_L e^{-j(\psi_a+\varphi_L)} \end{bmatrix} \tag{1}$$

The zero, positive and negative sequence components may be determined by using the method of symmetrical components.

$$\begin{bmatrix} \dot{I}^0 \\ \dot{I}^- \\ \dot{I}^+ \end{bmatrix} = \frac{1}{N_1}\begin{bmatrix} 1 & 1 & 1 \\ 1 & \alpha^2 & \alpha \\ 1 & \alpha & \alpha^2 \end{bmatrix}\begin{bmatrix} \dot{I}_a \\ \dot{I}_b \\ \dot{I}_c \end{bmatrix} = \frac{I_L}{N_1}\begin{bmatrix} 0 \\ \sqrt{3}e^{-j(\psi_a+\varphi_L+30^\circ)} \\ \sqrt{3}e^{-j(\psi_a+\varphi_L-30^\circ)} \end{bmatrix} \tag{2}$$

where $\alpha = e^{+j120^\circ}$. The unbalance factor of the currents in (1) is equal to 100% in terms of the definition in (3).

$$\text{Current unbalance factor} = \frac{|I^-|}{|I^+|} \times 100\% \tag{3}$$

According to the power quality standard [17], the voltage unbalance is estimated by (4), in which U_L is the

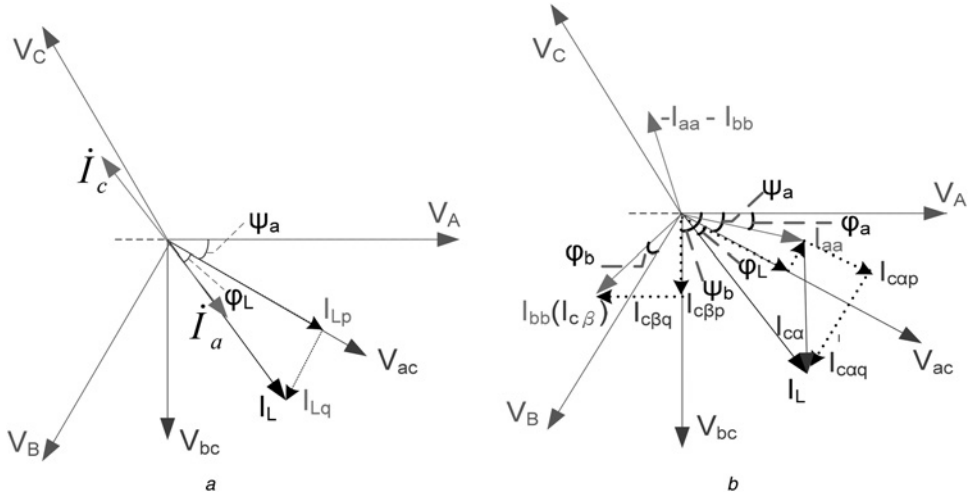

Fig. 2 *Phasor diagrams*

a Without RPC
b RPC operates

line-to-line voltage and S_k is the short-circuit capacity. In case the value of ε_U does not exceed 2%, the power quality standard is satisfied.

$$\varepsilon_U = \frac{\sqrt{3}|I^-|U_{\rm L}}{S_k} \times 100\% \tag{4}$$

2.2 Model with the RPC

A RPC is installed in the co-phase railway power supply, as shown in Fig. 1, which uses a back-to-back converter and injects currents to V_{ac} phase and V_{bc} phase, respectively. The corresponding phasor diagram is shown in Fig. 2*b*. After the single-phase RPC is installed, the currents at the secondary side of the traction transformer are expressed by (5), in which $I_{c\alpha}$ is the current injecting to the V_{ac} phase and $I_{c\beta}$ is the current injecting to the V_{bc} phase.

$$\begin{bmatrix} I_{aa} \\ I_{bb} \end{bmatrix} = \begin{bmatrix} I_{\rm L} - I_{c\alpha} \\ I_{c\beta} \end{bmatrix} \tag{5}$$

Each current is decomposed to the component in phase with its supply voltage and the component perpendicular to its supply voltage, which are denoted as p-axis component and q-axis component, respectively. As a result, (5) is revised as (6).

$$\begin{aligned} \begin{bmatrix} I_{aa} \\ I_{bb} \end{bmatrix} &= \begin{bmatrix} I_{aap} + {\rm j}I_{aaq} \\ I_{bbp} + {\rm j}I_{bbq} \end{bmatrix} \\ &= \begin{bmatrix} \left(I_{{\rm L}p} + {\rm j}I_{{\rm L}q}\right) - \left(I_{c\alpha p} + {\rm j}I_{c\alpha q}\right) \\ I_{c\beta p} + {\rm j}I_{c\beta q} \end{bmatrix} \end{aligned} \tag{6}$$

where

$$\begin{bmatrix} I_{aap} \\ I_{aaq} \\ I_{bbp} \\ I_{bbq} \end{bmatrix} = \begin{bmatrix} I_{{\rm L}p} - I_{c\alpha p} \\ I_{{\rm L}q} - I_{c\alpha q} \\ I_{c\beta p} \\ I_{c\beta q} \end{bmatrix} \tag{7}$$

The RPC absorbs active power from the V_{bc} phase and injects them to the V_{ac} phase. If the dc link voltage is kept as a constant value and the system losses are ignored, active power balance exists in the back-to-back converter as expressed by (8). Since $V_{ac} = \sqrt{3}V_A/N_1$ and $V_{bc} = \sqrt{3}V_A/N_1$, (9) is deduced.

$$V_{ac}I_{c\alpha p} = V_{bc}I_{c\beta p} \tag{8}$$

$$I_{c\beta p} = I_{c\alpha p} \tag{9}$$

The grid-side currents satisfy (10), since it is a three-phase three-wire system. As a result, the currents at the primary side of the traction transformer are given in (11) after the RPC is installed.

$$I_a + I_b + I_c = 0 \tag{10}$$

$$\begin{bmatrix} I_a \\ I_b \\ I_c \end{bmatrix} = \begin{bmatrix} \dfrac{1}{N_1} I_{aa} {\rm e}^{-{\rm j}\psi_a} \\ \dfrac{1}{N_1} I_{bb} {\rm e}^{-{\rm j}\psi_b} \\ -I_a - I_b \end{bmatrix} \tag{11}$$

2.3 Calculate compensating currents of the RPC

In previous studies, the references for controlling the output currents of the RPC are solved from a group of equations case by case in terms of compensation factors. However, the relationship between the compensation factors and the achieved PF after compensation is not deduced [13–15]. In this part, the current references are deduced by using the geometrical characteristics in the phasor diagrams.

According to (7) and (9), there are three unknown parameters, $I_{c\alpha p}$, $I_{c\alpha q}$ and $I_{c\beta q}$, for deducing the compensating currents. Both PF and negative sequence current at the grid side can be used as the condition for deducing them. Considering some utilities provide tariff plan varying with the PF, the PF at the high-voltage grid is selected and expressed in (12). It is defined that the phase angle in (12) is positive for inductive loads and is negative for capacitive loads. According to the geometrical characteristics in the phasor diagram in Fig. 2*b* and (9), (7) is revised as (13).

$$\begin{cases} \cos(\varphi_a) = {\rm PFA} \\ \cos(\varphi_b) = {\rm PFB} \\ \cos(\varphi_c) = {\rm PFC} \end{cases} \tag{12}$$

$$\begin{bmatrix} I_{aap} \\ I_{aaq} \\ I_{bbp} \\ I_{bbq} \end{bmatrix} = \begin{bmatrix} I_{{\rm L}p} - I_{c\alpha p} \\ \tan(\psi_a - \varphi_a)\left(I_{{\rm L}p} - I_{c\alpha p}\right) \\ I_{c\alpha p} \\ \tan\left(\psi_b - \dfrac{2}{3}\pi - \varphi_b\right) I_{c\alpha p} \end{bmatrix} \tag{13}$$

In (13), φ_a and φ_b are the power angle of phases A and B, as given in (12). ψ_a equals $\pi/6$ and it is the phase angle between the voltages V_{ac} and the grid-side voltage V_A. ψ_b is the angle between V_{bc} and V_A and $\psi_b = \pi/2$. In order to solve the unknown parameter $I_{c\alpha p}$, the PF at phase C is used. According to (11), the current at phase C is determined by the currents of phases A and B. The PF at phase C is given in (14). By substituting (13) to (14), $I_{c\alpha p}$ is deduced in (15).

$${\rm PFC} = \cos\left(\frac{2}{3}\pi - {\rm angle}\left(-\frac{1}{N_1} I_{aa} {\rm e}^{-{\rm j}\psi_a} - \frac{1}{N_1} I_{bb} {\rm e}^{-{\rm j}\psi_b}\right)\right) \tag{14}$$

(see (15))

With $I_{c\alpha p}$, the compensating currents of the RPC are

$$I_{c\alpha p} = \frac{\cos(\psi_b - \varphi_b - (2/3)\pi)\sin(\varphi_a - \varphi_c + (2/3)\pi)}{\cos(\psi_b - \varphi_b - (2/3)\pi)\sin(\varphi_a - \varphi_c + (2/3)\pi) + \cos(\psi_a - \varphi_a)\sin(\varphi_c - \varphi_b + (2/3)\pi)} I_{{\rm L}p} \tag{15}$$

doi: 10.1049/iet-pel.2013.0396

Table 1 Case study for different compensation settings

	PFA	PFB	PFC	Phase angle
case 1	inductive	inductive	inductive	$\varphi_a = \varphi_b = \varphi_c$
case 2	inductive	inductive	capacitive	$\varphi_a = \varphi_b = -\varphi_c$
case 3	inductive	capacitive	inductive	$\varphi_a = -\varphi_b = \varphi_c$
case 4	inductive	capacitive	capacitive	$\varphi_a = -\varphi_b = -\varphi_c$

current of RPC can be calculated in terms of the set PF at the grid. According to (17), the value of k is determined by the phase angles related to the traction transformer and the PF setting at the grid. However, for different types of the traction motor, the reactive power to be compensated varies. The load PF plays an important role in calculating the compensating currents in (16). The rating of the power

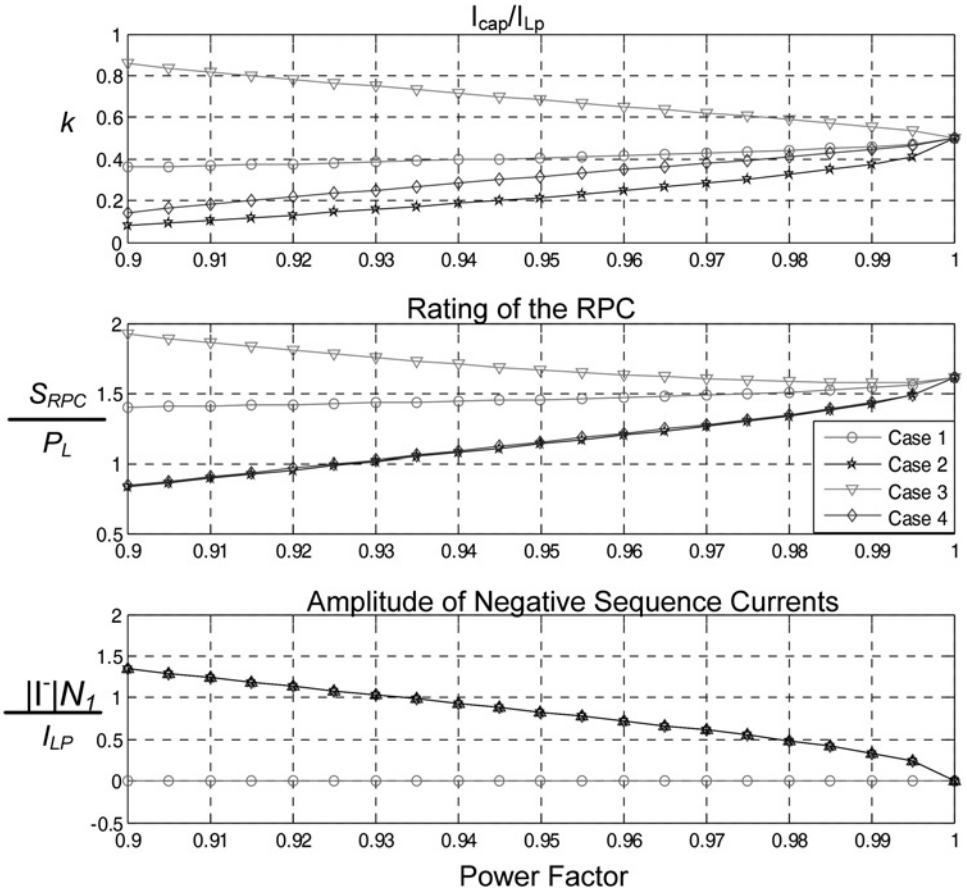

Fig. 3 *Comparisons of RPC rating for the four cases*

calculated by (16).

$$\begin{bmatrix} I_{c\alpha p} \\ I_{c\alpha q} \\ I_{c\beta p} \\ I_{c\beta q} \end{bmatrix} = \begin{bmatrix} I_{c\alpha p} \\ I_{Lq} - I_{aaq} \\ I_{bbp} \\ I_{bbq} \end{bmatrix} = \begin{bmatrix} k*I_{Lp} \\ -\tan(\varphi_L)I_{Lp} - \tan(\psi_a - \varphi_a)(1-k)I_{Lp} \\ k*I_{Lp} \\ \tan\left(\psi_b - \frac{2}{3}\pi - \varphi_b\right)*k*I_{Lp} \end{bmatrix} \quad (16)$$

where (see (17))

Equations (16) and (17) indicate that the compensating converters in the RPC is defined by (18).

$$S_{RPC} = \frac{\sqrt{3}V_A}{N_1}\sqrt{I_{c\alpha p}^2 + I_{c\alpha q}^2} + \frac{\sqrt{3}V_A}{N_1}\sqrt{I_{c\beta p}^2 + I_{c\beta q}^2} \quad (18)$$

Substitute (16) to (18), the normalised rating of the RPC is given in (19). The denominator is the active power of the traction load.

$$\frac{S_{RPC}}{\sqrt{3}V_A I_{Lp}/N_1} = \frac{S_{RPC}}{P_L} = \left(\sqrt{k^2 + \left(\tan(\varphi_L) + \tan(\psi_a - \varphi_a)(1-k)\right)^2} + k\sqrt{1 + \left(\tan\left(\psi_b - \frac{2}{3}\pi - \varphi_b\right)\right)^2}\right) \quad (19)$$

$$k = \frac{I_{c\alpha p}}{I_{Lp}} = \frac{\cos(\psi_b - \varphi_b - (2/3)\pi)\sin(\varphi_a - \varphi_c + (2/3)\pi)}{\cos(\psi_b - \varphi_b - (2/3)\pi)\sin(\varphi_a - \varphi_c + (2/3)\pi) + \cos(\psi_a - \varphi_a)\sin(\varphi_c - \varphi_b + (2/3)\pi)} \quad (17)$$

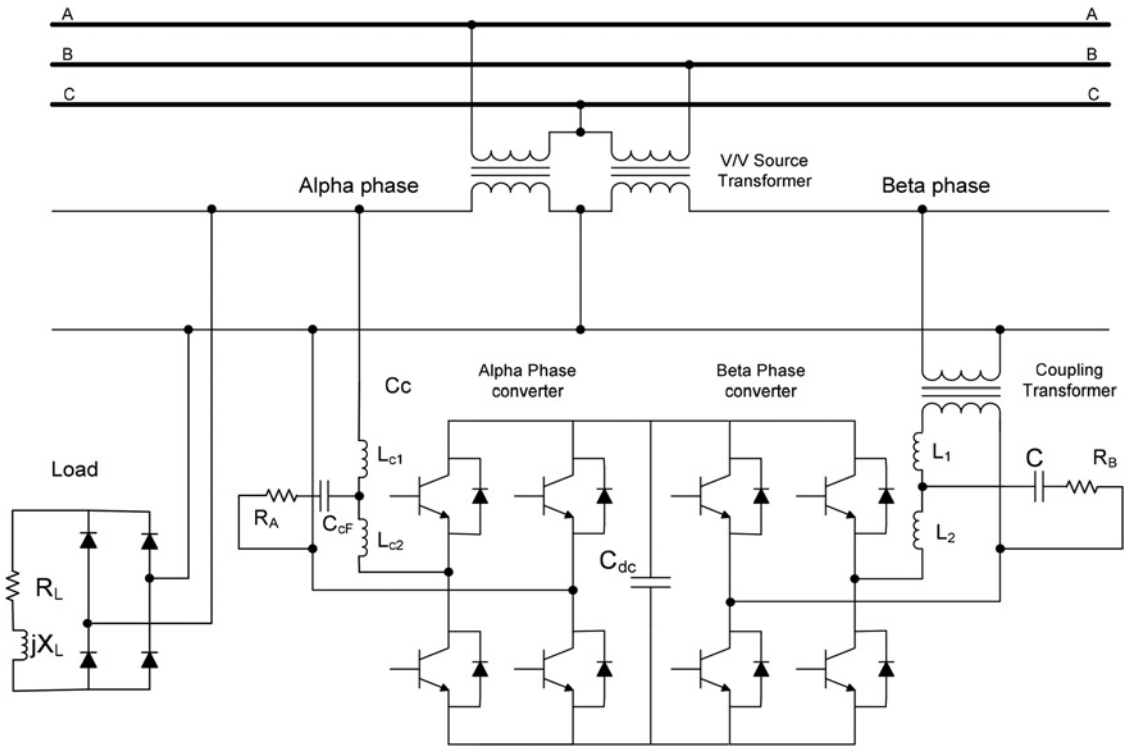

Fig. 4 *Topology of the single-phase RPC*

The above analyses calculate the compensating currents in terms of the achieved PF at the grid side. After the compensating currents are determined, the negative sequence currents at the grid side still need to be evaluated by the unbalance standard. According to (4), if the negative sequence current is smaller than the threshold value in (20), the system unbalance satisfies the standard. The negative sequence currents after compensation can be calculated by substituting (11) into (21).

$$|I^-| \le \frac{S_k \varepsilon_U}{\sqrt{3}U_L} = \frac{S_k \cdot 2\%}{\sqrt{3}U_L} \tag{20}$$

$$|\dot{I}^-| \cdot N_1 = |(\dot{I}_a + \alpha^2 \dot{I}_b + \alpha \dot{I}_c)| \tag{21}$$

3 Design and implementation of a reduced rating RPC

3.1 Design of the RPC

Analyses in the previous section provide a method to calculate the required compensating currents in terms of the PF after compensation. How to set the PF to achieve the minimum power rating of the RPC is first studied. It is preferred to set same PF for the phases *A*, *B* and *C*, so that the PF of the three-phase grid is the same as the PF of each phase, as illustrated in (22).

$$\mathrm{PF}_{\mathrm{grid}} = \frac{P_A + P_B + P_C}{S_A + S_B + S_C} \tag{22}$$

The reactive power can be either inductive or capacitive and the PF in (22) is not affected. Since the traction loads are inductive, it is clear from Fig. 2*b* that the PF after compensation should be inductive at phase *A* in order to reduce the compensating currents at the V_{ac} phase. However, the PF at phases *B* and *C* can be set inductive or capacitive. It is difficult to straightforwardly determine a setting combination which would result in lower compensating current**.** Hence, four groups of the PF settings in Table 1 are compared.

It is assumed the penalty for the reactive power is applied when the PF is < 0.9 [19–21]. The PF is set to vary from 0.9 to 1. The load PF is assumed to be 0.85. The variations of the following three parameters in terms of setting in Table 1 are shown in Fig. 3.

- The parameter k calculated by (17), which is used to calculate the compensating currents of the RPC;
- The required rating of the RPC is calculated by (19);
- The amplitude of the negative sequence current at the grid side is calculated by (21).

Fig. 3 indicates that cases 2 and 4 in Table 1 achieve the lowest RPC rating when the grid PF reaches the set value. In case 3, the required rating is even higher than that of the full compensation, which is the worst case. Fig. 3 pointed out the important characteristic that the compensator ratings can vary in a large range by setting different k values and leading or lagging phase angles in different phases. Case 1 balances the currents at the grid even the PF is not unity. When the traction substation is designed, the short-circuit capacity is selected to allow certain unbalance currents flow inside the system. As a result, cases 2 and 4 are considered for designing a reduced rating RPC. As shown in Fig. 3, the k value of case 2 is smaller than that of case 4. This parameter corresponds to the active component of the compensating current at the V_{ac} phase. Smaller k means less active power is transferred via the back-to-back converter of the RPC. Hence the case 2 is selected for setting the PF.

doi: 10.1049/iet-pel.2013.0396

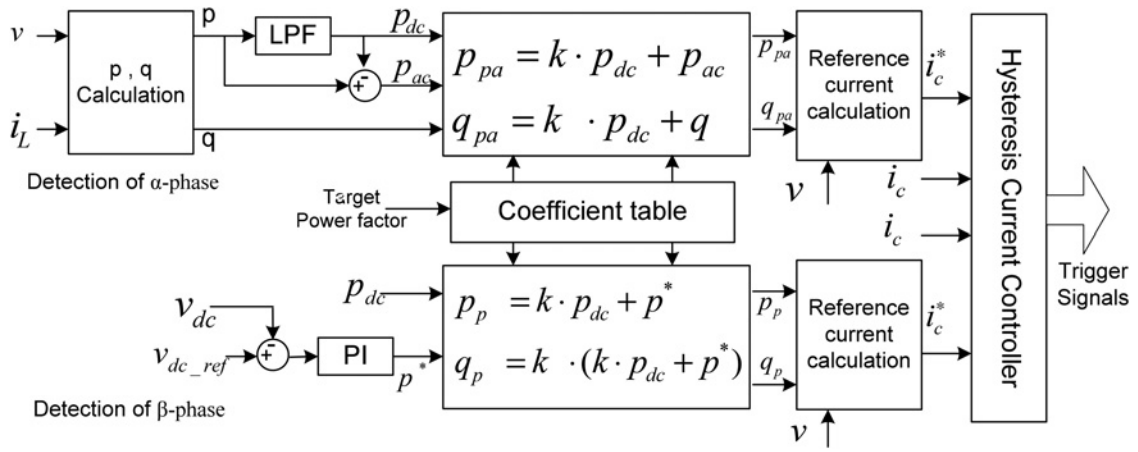

Fig. 5 *Control system of the RPC*

Table 2 Circuit parameters of RPC in simulation

No.	Items	Description
1	α-phase coupling inductor L_{C1}, L_{C2}	3.3 mH
2	α-phase C_{CF}	10 μF
3	α-phase R_A	15 Ω
4	dc capacitor C_{dc}	10 000 μF
5	β-phase L_1, L_2	2 mH
6	β-phase C	10 μF
7	β-phase R_B	25 Ω
8	dc link voltage	40 kV

When the RPC is designed, the PF is set according to the utility tariff plan for the reactive power. For example, PF is at least 0.9 in order to avoid penalty. For different types of the traction motor, the corresponding PF is substituted to (19) to design the RPC's rating. More reactive power needs to be compensated during the motor starting. To cope with this particular case, it is better to overdesign the reactive power compensation capability. A safety margin is required considering possible over-loading, 0.95 is used as the PF to design the RPC in this paper. The rating of the RPC is reduced to 70% of the value when the RPC is designed to achieve unity PF according to Fig. 3. By applying the new design method, not only the rating of the power converters, but also the rating of the coupling transformer and other passive components are reduced. This greatly reduces the initial cost of the RPC. At the same time, the operational loss of the RPC is reduced since it is proportional to the compensating currents, which include the switching losses, copper losses etc.

3.2 Implement control system of the RPC

The topology of a co-phase power supply system with a RPC is shown in Fig. 4. The α-phase converter is connected in parallel to the traction loads and the β-phase converter is connected to the other output of the V/V transformer via a single-phase isolation transformer. A single-phase full-bridge back-to-back converter is adopted for illustrating the operational principle of the proposed system. For the isolation purpose, only one isolation transformer is required at the two terminals of the RPC. Practically, a multi-level converter is a better alternative when the α-phase converter of the RPC is connected to the supply without coupling transformer [22, 23].

The control system block diagram is given in Fig. 5. The RPC transfers active power from β-phase to α-phase. The α-phase converter also works for reactive power compensation and harmonic suppression. The β-phase converter works for dc-bus voltage control. In order to calculate the reference currents in (16), the instantaneous power method is used. The instantaneous active and reactive power is calculated by (23), in which $v_{\alpha d}$ and $i_{\alpha d}$ are 90° delay of the system voltage and load current, respectively. The injecting power from the RPC is

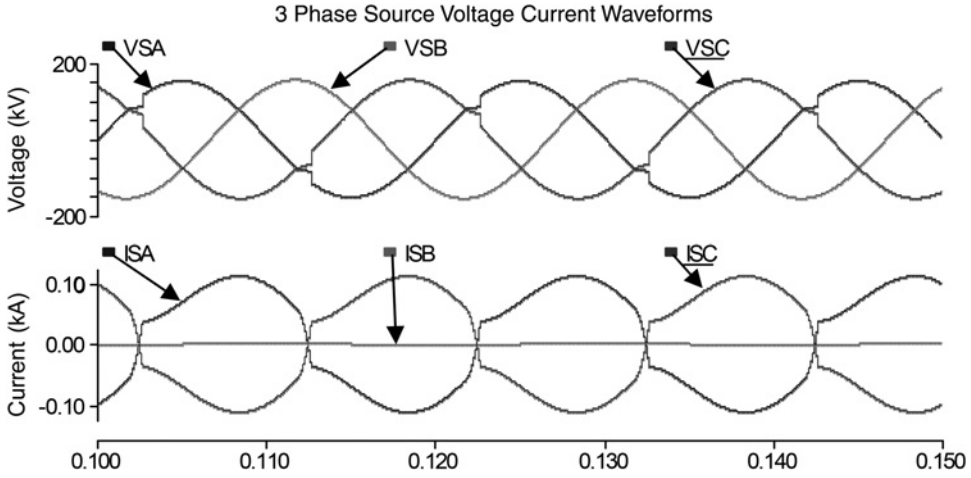

Fig. 6 *Grid-side voltages and currents without RPC*

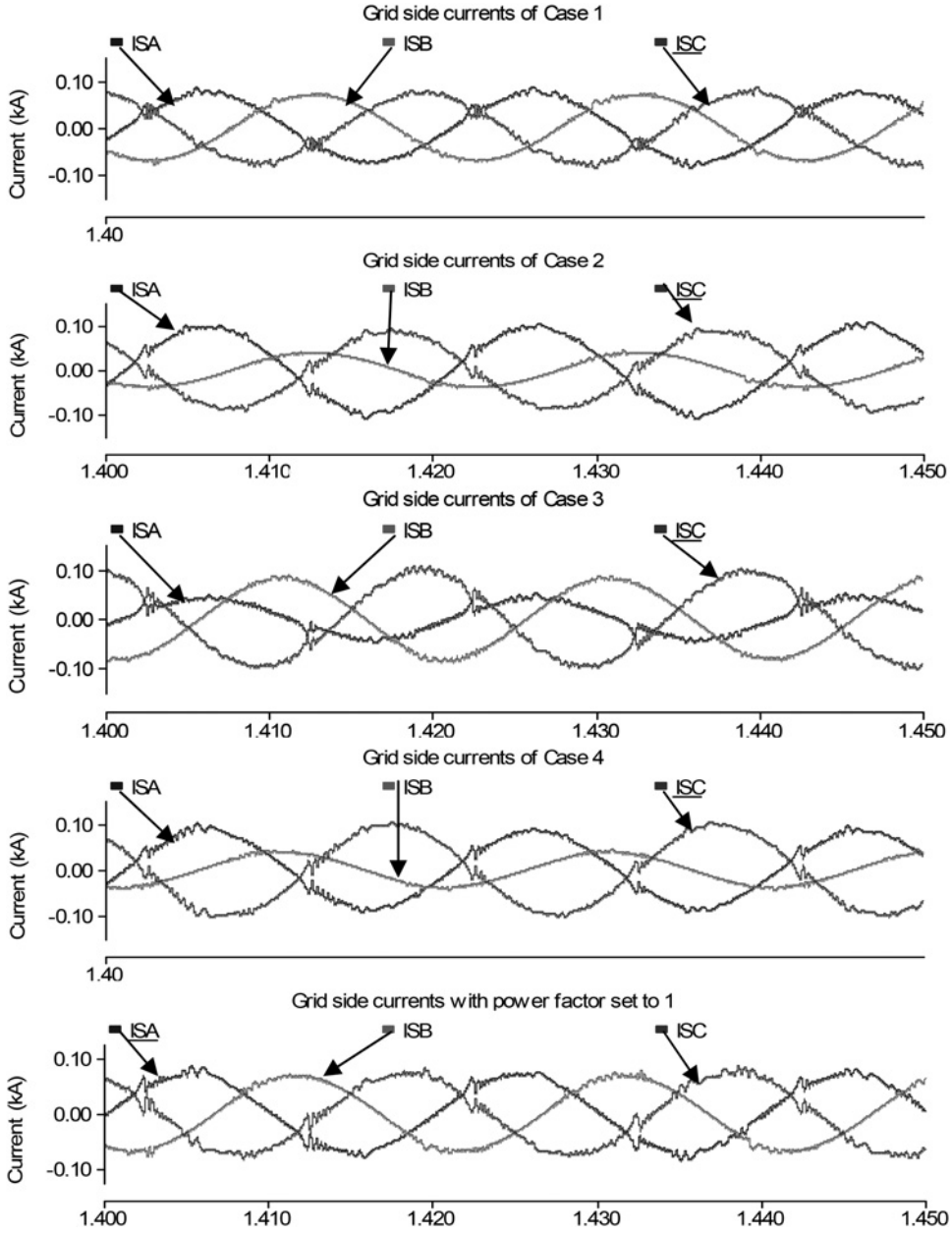

Fig. 7 *Grid-side currents with RPC under partial compensation (four cases in Table 1) and full compensation*

calculated as given in (24) in terms of the compensating current in (16).

$$\begin{bmatrix} p \\ q \end{bmatrix} = \begin{bmatrix} v_\alpha \cdot i_{\mathrm{L}} + v_{\alpha d} \cdot i_{\mathrm{L}d} \\ v_\alpha \cdot i_{\mathrm{L}d} - v_{\alpha d} \cdot i_{\mathrm{L}} \end{bmatrix} \tag{23}$$

$$\begin{bmatrix} p_{p\alpha} \\ q_{pa} \\ p_{p\beta} \\ q_{p\beta} \end{bmatrix} = \begin{bmatrix} k \cdot p_{\mathrm{dc}} + p_{ac} \\ k_\alpha \cdot p_{\mathrm{dc}} + q \\ k \cdot p_{\mathrm{dc}} + p^* \\ k_\beta \cdot (p_{\mathrm{dc}} \cdot k + p^*) \end{bmatrix} \tag{24}$$

Table 3 Comparison of four cases in Table 1 and full compensation

Setting	Grid-side PF			Grid-side current RMS, A			Output current RMS of RPC, A		Voltage unbalance, %
	A	*B*	*C*	*A*	*B*	*C*	$I_{c\alpha}$	$I_{c\beta}$	
without RPC	0.65	—	0.98	84.3	0	84.3	0	0	2.13
case 1 (PF = 0.95)	0.948	0.955	0.967	53.1	50.3	53.8	331.4	348.6	0.156
case 2 (PF = 0.95)	0.945	0.959	0.953	69.7	27.4	62.7	302.6	189.7	1.13
case 3 (PF = 0.95)	0.952	0.951	0.964	29.8	57.9	68.0	426.3	401.0	0.96
case 4 (PF = 0.95)	0.943	0.952	0.955	60.3	28.6	70.3	311.8	198.4	1.11
full compensation	1.00	1.00	1.00	50.4	48.7	51.5	437.4	337.4	0.123

doi: 10.1049/iet-pel.2013.0396

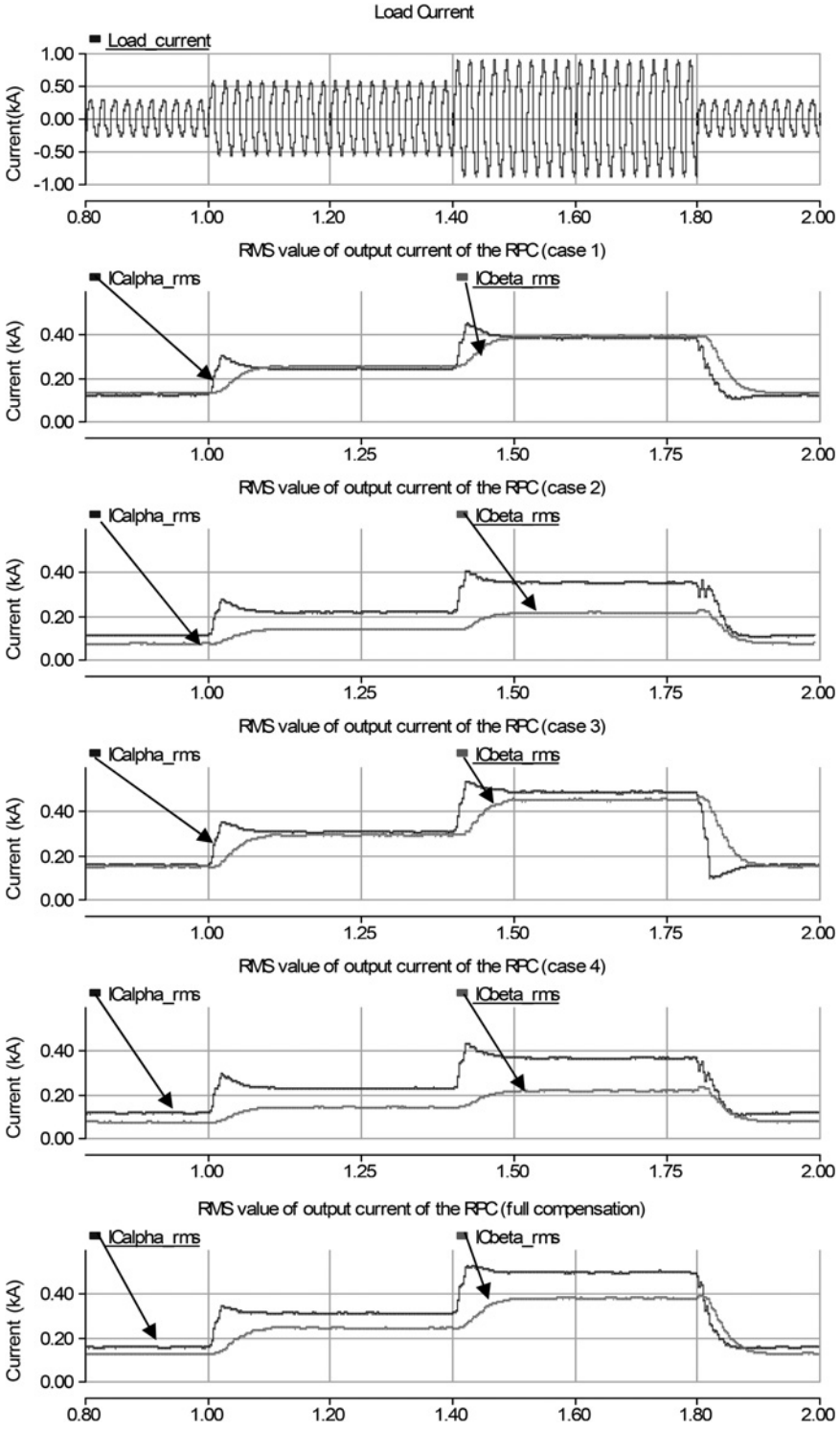

Fig. 8 *Load currents and output currents of the RPC in terms of four cases in Table 1 and full compensation*

Table 4 Compensation performance of the RPC by case 2

	Grid-side PF			Grid-side current RMS, A			Output current of RPC, A		Voltage unbalance, %
	A	*B*	*C*	*A*	*B*	*C*	$I_{c\alpha}$	$I_{c\beta}$	
without RPC	0.65	—	0.98	84.3	0	84.3	0	0	2.13
set PF = 0.9	0.896	0.924	0.910	79.3	12.6	75.0	241.9	87.0	1.75
set PF = 0.92	0.916	0.933	0.925	75.5	18.5	69.4	258.8	128.0	1.49
set PF = 0.95	0.945	0.959	0.953	69.7	27.4	62.7	302.6	189.7	1.13
set PF = 0.98	0.977	0.982	0.977	62.1	36.1	55.7	353.1	250.3	0.70
set PF = 1.0	1.00	1.00	1.00	50.4	48.7	51.5	437.4	337.4	0.123

Table 5 Circuit parameters in experiment

No.	Items	Description
1	α-phase coupling inductor L_a	4 mH
2	α-phase coupling capacitor C_a	170 μF
3	C_{dx}	5000 μF
4	coupling transformer T	1:2, 2 kVA
5	β-phase coupling inductor	4.7 mH

where $k_\alpha = -\tan(\psi_a - \phi_a)(1-k)$ and $k_\beta = \tan(\psi_b - (2/3)\pi - \phi_b)$. The coefficients k, k_α and k_β are got from a coefficient table in terms of the PF target at the grid.

4 Simulation verification

Simulations are done by using PSCAD/EMTDC. The system configuration is shown in Fig. 4 and parameters are given in Table 2. The short-circuit capacity of the 110 kV supply is

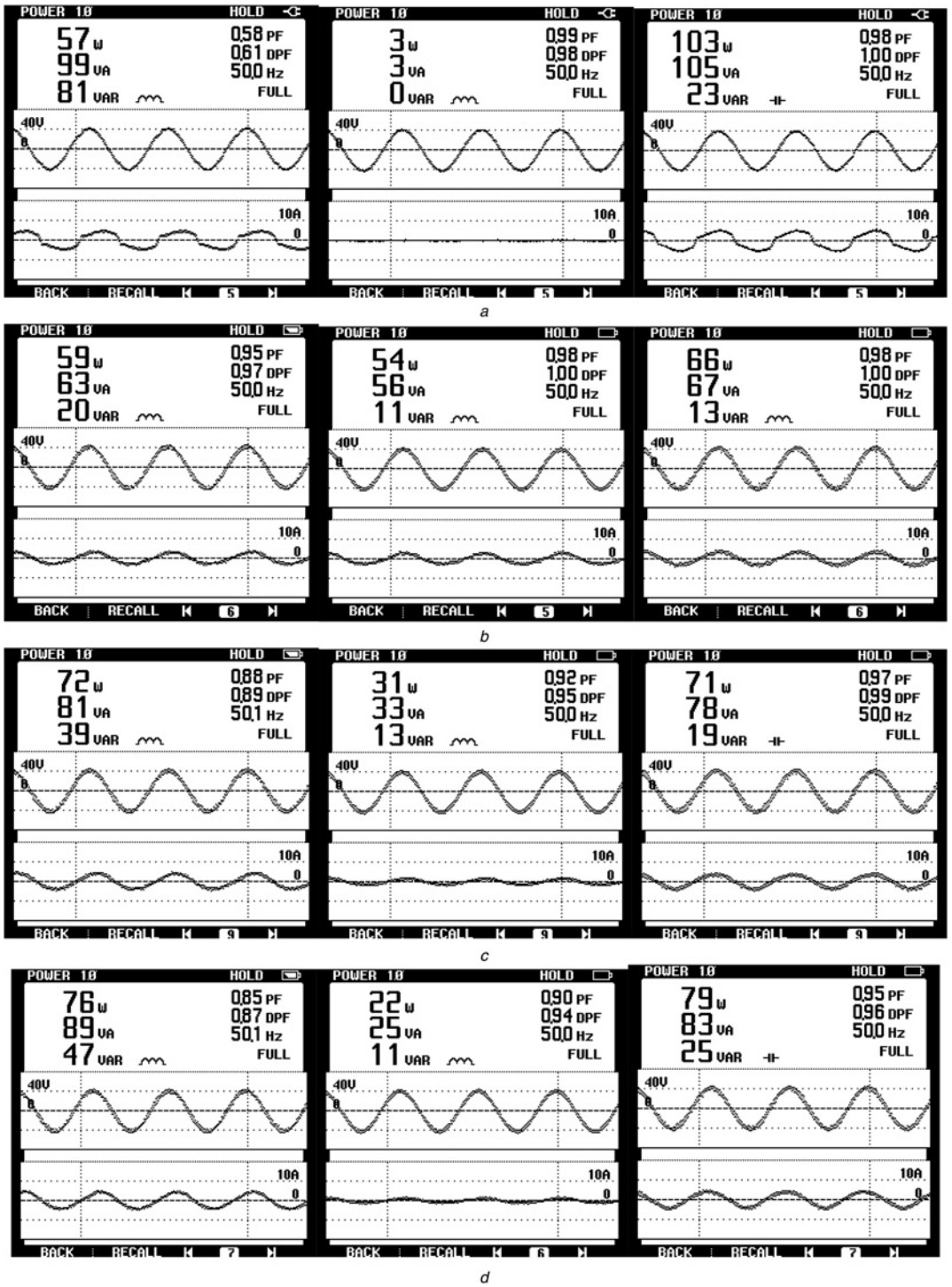

Fig. 9 *Experimental results*

a Without RPC
b PF set to 1
c PF set to 0.95
d PF set to 0.92

doi: 10.1049/iet-pel.2013.0396

Table 6 Experimental results of the RPC by case 2

	Grid-side PF			Output current of RPC, A		Grid-side current RMS, A		
	A	*B*	*C*	$I_{c\alpha}$	$I_{c\beta}$	*A*	*B*	*C*
without RPC	0.58	—	0.98	0	0	3.822	0	3.85
set PF = 0.92	0.87	0.94	0.96	1.66	0.85	3.05	0.85	2.87
set PF = 0.95	0.89	0.95	0.99	1.85	1.13	2.78	1.13	2.58
set PF = 1.0	0.97	1.00	1.00	2.56	1.92	2.13	1.92	2.34

750 MVA. One 20 MVA 110 kV/27.5 kV V/V transformer is used to supply the traction load. The LCL filter is designed according to the method employed in [24, 25]. The traction loads are modelled by a single-phase rectifier with inductive loads.

Without the RPC, the voltage and current at the primary side of the traction transformer are shown in Fig. 6. The phase angles according to four cases in Table 1 are substituted to (24) to calculate the reference currents when the PF is set to 0.95. The grid-side currents are shown in Fig. 7 after the RPC injecting currents to the system. It could be observed that the RPC compensates the harmonics simultaneously when it balance the grid-side currents and compensate reactive power. The result of full compensation is also included in Fig. 7 and Table 3. In the worst case 3, the required rating under partial compensation is even higher than that under full compensation. The case 2 achieves the minimum RPC rating by setting the power angle of phases *A* and *B* lagging and the power angle of phase *C* leading. This conclusion can also be deduced from Fig. 8 when dynamic loads are tested. Traction load current and compensating current from RPC are shown in Fig. 8.

Since case 2 achieves the minimum RPC rating, its setting is selected. Five different pre-set PF at the grid side in case 2 are tested and the results are summarised in Table 4. According to the power quality standards [17, 26], the voltage unbalance should be $<2\%$. The voltage unbalance is $<2\%$ in Table 4 after the RPC operates. For a higher pre-set PF, the voltage unbalance after compensation is lower. The rating of the RPC is reduced to $<70\%$ when PF is set to 0.95 instead of 1. As a result, the full compensation with high initial cost is not necessary.

5 Experimental verification

A small capacity co-phase railway power supply with the RPC was built for verification. The system configuration is the same as Fig. 4. The V/V traction transformer is composed of 1:1 isolation transformers, with capacity of 5 kVA individually. The peak value of the single-phase supply voltage at the secondary side of the transformer is around 70 V and the dc link voltage of the RPC is 80 V. The total capacity of the experimental prototype is greatly reduced compared with the simulation models. The LCL filter in Fig. 4 is replaced by an inductor since the filtering requirement of small capacity system is lower. The circuit parameters in experiment are listed in Table 5. The traction loads are modelled by a single-phase rectifier with inductive loads.

The experimental results are shown in Fig. 9. Fig. 9*a* shows the voltages and currents waveforms at the three-phase grid sides without the RPC operating. The corresponding PF and current RMS values are listed in Table 6. The control system is set to achieve the grid-side PF of 1, 0.95 and 0.92, respectively. The experimental results for each case are recorded. After the RPC operates, the voltages and currents at the grid are shown in Figs. 9*b–d* and the performance indexes are listed in Table 6. The grid-side PF is improved to approach the PF setting. With a lower PF target, the required compensating currents from the RPC are also lower. Since the dc voltage of the three cases is the same, the compensating currents directly determine the required capacity of the power converters in the RPC. The experimental results also validate the proposed design and control method.

6 Conclusions

In this paper, the mathematical model of the co-phase traction power system with the RPC is studied. By using the geometrical properties, the relationship between the compensating currents and the achieved grid-side PF is deduced. The RPC can adopt different control approaches to reach the same PF based on the mathematical model. On taking the PF setting to 0.9 as an example, the rating of the RPC in the worst case is more than twice that in the best case. Selection of a suitable control parameter to reduce the RPC rating is studied. The minimum rating of the RPC is achieved by setting the power angle of phases *A* and *B* lagging and the power angle of phase *C* leading under partial compensation. The control block of the reduced rating RPC is implemented. The rating of the RPC is reduced by 30%, in case the PF after compensation is set to 0.95 instead of 1. As a result, the initial cost and operational losses of the RPC is reduced. Simulation and experimental results indicate that the RPC can compensate the reactive current, harmonics and current unbalance simultaneously. It is also validated that the PF can be improved to the set target and the rating of the RPC is reduced accordingly.

7 Acknowledgments

The authors thank the Science and Technology Development Fund, Macao SAR Government under the project 015/2008/A1 and Research Committee of University of Macau for their financial support.

8 References

1 Kneschke, T.A.: 'Control of utility system unbalance caused by single-phase electric traction', *IEEE Trans. Ind. Appl.*, 1985, **IA-21**, (6), pp. 1559–1571

2 Han, Z., Zhang, Y., Liu, S., Gao, S.: 'Modeling and simulation for traction power supply system of high-speed railway'. Proc. of Power and Energy Engineering Conf. (APPEEC), 2011, pp. 1–4

3 Raygani, S.V., Tahavorgar, A., Fazel, S.S., Moaveni, B.: 'Load flow analysis and future development study for an AC electric railway', *IET Electr. Syst. Transp.*, 2012, **2**, (3), pp. 139–147
4 Dai, C., Sun, Y.: 'Investigation of the imbalance current compensation for transformers used in electric railways'. 2010 Asia-Pacific Power and Energy Engineering Conference (APPEEC), 2010, pp. 1–4
5 Liu, Y., Wu, G., Hua, H., Wang, L.: 'Research for the effects of high-speed electrified railway traction load on power quality'. Proc. Fourth Int. Conf. on Electric Utility Deregulation and Restructuring and Power Technologies (DRPT), 2011, pp. 569–573
6 Tan, P.-C., Loh, P.C., Holmes, D.G.: 'Optimal impedance termination of 25-kV electrified railway systems for improved power quality', *IEEE Trans. Power Deliv.*, 2005, **20**, (2), pp. 1703–1710
7 Gholizad, B., Akhbari, M.: 'A topology of hybrid active power filter for simultaneously compensating harmonics and load unbalance in single phase traction systems'. Conf. on Power Engineering, Energy and Electrical Drives, 2011, pp. 1–6
8 Chen, M., Li, Q., Wei, G.: 'Optimized design and performance evaluation of new cophase traction power supply system'. Power and Energy Engineering Conference, 2009 (APPEEC 2009), Asia-Pacific, 2009, pp. 1–6
9 Shu, Z., Xie, L., Li, Q.: 'Single-phase back-to-back converter for active power balancing, reactive power compensation and harmonic filtering in traction power system', *IEEE Trans. Power Electron.*, 2011, **26**, (2), pp. 334–343
10 Zhou, F., Li, Q., Qiu, D.: 'Co-phase traction power system based on balanced transformer and hybrid compensation'. Proc. Asia-Pacific Power and Energy Engineering Conference (APPEEC), 2010, pp. 1–4
11 Dai, N.Y., Lao, K.W., Wong, M.C., Wong, C.K.: 'Hybrid power quality conditioner for co-phase power supply system in electrified railway', *IET Power Electron.*, 2012, **5**, (7), pp. 1084–1094
12 Lao, K.-W., Dai, N.Y., Liu, W.-G., Wong, M.-C.: 'Hybrid power quality compensator with minimum DC operation voltage design for high speed traction power systems', *IEEE Trans. Power Electron.*, 2013, **28**, (4), pp. 2024–2036
13 Zhang, L., Li, Q., Zhou, X.: 'The optimal configuration of reactive compensating capacity for traction substation'. Proc. 2009 Asia-Pacific Power and Energy Engineering Conference (APPEEC), 2009, pp. 1–5
14 Zou, D., Li, Q., Zhang, L.: 'The design of comprehensive compensation in traction substation based on measured data'. Proc. 2010 Asia-Pacific Power and Energy Engineering Conference (APPEEC), 2010, pp. 1–4
15 Chuanping, W., An, L., Xianyong, X.: 'Integrative compensation method of negative phase sequence and harmonic for high-speed railway traction supply system with V/V transformer', *Proc. CSEE*, 2010, **30**, (6), pp. 111–117
16 IEEE Std 519–1992: 'IEEE recommended practices and requirements for harmonic control in electrical power systems', 1992
17 GB/T 15543–2008: 'Power quality – three-phase voltage unbalance', National Standard of the People's Republic of China, 2008
18 IEEE Std C57.110–1998: 'IEEE recommended practice for establishing transformer capability when supplying nonsinusoidal load currents', 1998
19 The Ministry of Water Resources and Electric Power: 'Power-factor regulating tariff measures', 1983
20 Tang, Y.S., Jiang, K., Zhong, J.Q.: 'Suggestion about revising power-factor regulating tariff measures', *Demand Side Manage.*, 2006, **8**, (3), pp. 22–24
21 Tang, Y.S., Zhuang, Z., Li, X.H.: 'Reasoning report about 'power-factor regulating tariff measures' amending', *South. Power Syst. Technol.*, 2009, **3**, (2), pp. 42–45
22 Song, Q., Liu, W.H.: 'Control of a cascade STATCOM with star configuration under unbalanced conditions', *IEEE Trans. Power Electron.*, 2009, **24**, (1), pp. 45–48
23 Akagi, H.: 'Classification, terminology, and application of the modular multilevel cascade converter (MMCC)', *IEEE Trans. Power Electron.*, 2011, **26**, (11), pp. 3119–3130
24 Wu, W., He, Y., Blaabjerg, F.: 'An LLCL power filter for single-phase grid-tied inverter', *IEEE Trans. Power Electron.*, 2012, **27**, (2), pp. 782–780
25 He, J., Li, Y.W., Bosnjak, D., Harris, B.: 'Investigation and active damping of multiple resonances in a parallel-inverter based microgrid', *IEEE Trans. Power Electron.*, 2013, **28**, (1), pp. 234–246
26 IEEE Std. 1159–1995: 'IEEE recommend practice for monitoring electric power quality', 1995

doi: 10.1049/iet-pel.2013.0396